JOURNAL OF OPTOELECTRONICS AND ADVANCED MATERIALS Vol. 9, No. 11, November 2007, p. 3604 - 3608

Optical, structural and electrical properties of ultrasonically sprayed copper oxide films: the effect of Mg incorporation

F. ATAY*, V. BILGIN, I. AKYUZ, S. KOSE
Department of Physics, Eskisehir Osmangazi University, 26480 Eskisehir, Turkey

In this work, undoped and Mg doped (at the Mg percentages of 1, 3 and 5) copper oxide films were deposited at the substrate temperature of 300±5 °C by ultrasonic spray pyrolysis technique, and the effect of Mg incorporation on the optical, structural and electrical properties was presented. Optical properties of the films were analyzed by transmission, linear absorption coefficient and reflection spectra, and the optical method was used to determine the band gaps of the films. The film structures were studied by X-ray diffraction, and the texture coefficient (P), the grain size (D), and macrostrain (<e>) for preferential orientations were calculated. The electrical conductivities were calculated with two-probe technique. Consequently, it was determined that Mg incorporation has a strong effect on the optical and especially structural properties of the copper oxide films.

(Received July 11, 2007; accepted November 1, 2007)

Keywords: Copper oxide films; Ultrasonic spray pyrolysis; Electrical and optical properties, XRD, UV

1. Introduction

Copper oxide, $CuAlO_2$, $CuGaO_2$ and $SrCu_2O_2$ are known to show p-type conductivity, and the development of these p-type semiconductors is one of the key technologies for pn-junction-based devices such as diodes, transistors and light-emitting diodes [1-3]. Among these materials, copper oxide films have unique features such as their low cost, non-toxicity, the abundant availability of copper, a theoretical solar cell efficiency of 18% and relatively simple formation of the oxide layer [4]. Copper oxide has two common forms as cupric oxide or tenorite (CuO, a band gap of 1.9–2.1 eV and a monoclinic structure) and cuprous oxide or cuprite (Cu_2O, a band gap of 2.1–2.6 eV and a cubic structure) [5-7]. Copper oxide-based materials are of interest on account of their potential uses in many technological fields, and they are potentially useful for constructing junction devices. Apart from these applications, these materials have been employed as heterogenous catalysts for several environmental processes, solid state gas sensor heterocontacts and microwave dielectric materials and as electrode materials for lithium batteries [8-10].

Copper oxide films have been prepared using various deposition techniques such as reactive magnetron sputtering [6], reactive evaporation [7], RF sputtering [4], ion beam sputtering [11], plasma evaporation [12], sol–gel [13,14], molecular beam epitaxy [15], spin coating [16] and solid-state reaction [17].

The aim of this work is to observe the effect of Mg incorporation on the optical, structural and electrical properties of ultrasonically sprayed copper oxide films and to investigate the feasibility of the films for solar cell devices as absorbing layers.

2. Experimental details

Copper oxide and Mg-incorporated (at 1%, 3% and 5%) copper oxide films were deposited onto glass substrates (objekttrager, 1×1 cm^2) by the ultrasonic spray pyrolysis (USP) technique at a substrate temperature of 300±5 °C. Details of the USP technique were given in our previous works [18, 19]. The ultrasonic frequency was 100 kHz, and the droplet size was 20 μm. The spraying solution was prepared by dissolving $Cu(CH_3COO)_2.2H_2O$ (0.1 M) and $Mg(CH_3COO)_2.2H_2O$ (0.1 M) in distilled water. The total solution (75 ml) was sprayed during 15 mins, and the solution flow rate was controlled by a flowmeter and kept at 5 $ml.min^{-1}$. Compressed purified air was used as the carrier gas (1 bar). The substrates were heated by an electrical heater, and the substrate temperature was measured using an iron-constantan thermocouple. The distance between the nozzle and the substrate was maintained at 30 cm. The produced films were named as BM0, BM1, BM3 and BM5 depending on the increasing Mg incorporation amount. The thicknesses of the films were measured using Metallurgical Optical Microscope. The codes and thicknesses of the copper oxide films are given in Table 1. It was seen from Table 1 that the thicknesses of the copper oxide thin films decrease depending on the increasing Mg incorporation. Optical transmissions and absorptions of the films were recorded by a Perkin Elmer UV/VIS Lambda 2S spectrometer (double–beam).The crystalline structure of the copper oxide thin films was confirmed by x-ray diffraction (XRD) with CuK_α radiation (Rigaku model, λ=1.5406 Å). Current-voltage (I-V) measurements were done in the dark by using a Keithley 485 Autoranging Picaommeter and Philip Harris 5kV Supply d.c gauge.

Table 1. The codes and thicknesses of the copper oxide films.

Material	Code	Thickness (μm)
Copper oxide	BM0	0.93
Mg incorporated copper oxide (at 1 %)	BM1	0.90
Mg incorporated copper oxide (at 3 %)	BM3	0.83
Mg incorporated copper oxide (at 5 %)	BM5	0.82

3. Results and discussion

3.1. Optical properties

The transmission spectra were taken at room temperature in air and are shown in Fig. 1. It was determined that all films behaved as transparent materials at about 800-1100 nm wavelength range. The transmittance values of the films decreased sharply at about wavelengths less than 800 nm because of their highly absorbing properties. This wavelength range represents to the fundamental absorption region. Besides, as seen in Fig. 1, the optical transmissions of the BM0 films were approximately 60% in the visible region, and these high transmission values decreased for BM1 and BM3 films and increased for BM5 films. This effect of Mg incorporation on the transmission of the copper oxide films may be due to the structural properties, surface smoothness and defect density.

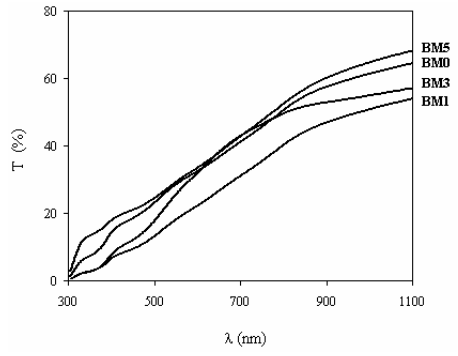

Fig. 1.The transmission spectra of the copper oxide films.

The linear absorption coefficient (α=A/d; where A is the absorbance and d is the thickness of the films) spectra of the copper oxide films are shown in Fig. 2. As seen in Fig. 2, BM1 and BM3 films have high absorption coefficients because of their lower transmissions. The reflectivity (R) of the copper oxide films can be calculated using the transmittance (T) and absorbance (A) spectra from the expression [20, 21],

$$T = (1-R^2)\exp(-A) \quad (1)$$

The reflection spectra of the copper oxide films are shown in Fig. 3. It was clearly seen that the reflection values are high in the visible region, and the values of the BM5 films are low. The increase of the reflection values for BM1 and BM3 films can be interpreted as follows. From the XRD analyses, we determined that BM1 and BM3 films consisted of Cu_2O and CuO phases, and the peak intensities of the Cu_2O phases are dominant. The Cu_2O is cubic and optically isotropic, while the CuO crystalline is monoclinic, biaxial and optically anisotropic. The crystalline of optically anisotropic monoclinic structure causes the double refraction. The double refraction in a polycrystalline film brings about the light scatterings [22]. So, we think that the high reflection values in BM1 and BM3 films is due to the scatterings of light from the optically anisotropic monoclinic structure (CuO).

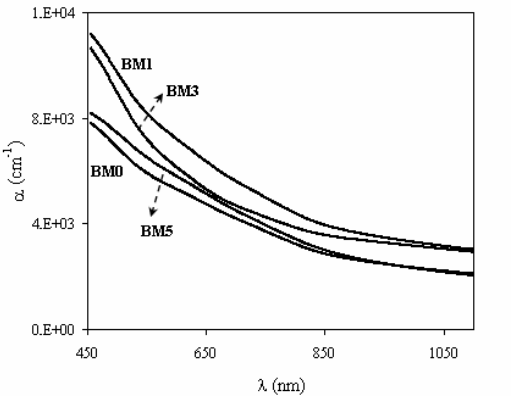

Fig. 2.The linear absorption coefficient spectra of the copper oxide films.

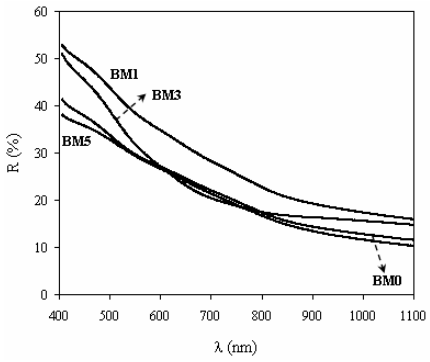

Fig. 3.The reflection spectra of the copper oxide films.

The refractive index (n) and the extinction coefficient (k) of the copper oxide films are given by the formulas [21],

$$k = \frac{\alpha \lambda}{4\pi} \quad (2)$$

$$n = \frac{1+R}{1-R} + \sqrt{\frac{4R}{(1-R)^2} - k^2} \quad (3)$$

The transmission (T), reflection (R), linear absorption coefficient (α) and refractive index (n) values of the copper oxide films are given in Table 2. It was clearly seen that Mg incorporation has a little effect on the optical properties of the copper oxide films.

Table 2. *The transmission (T), reflection (R), linear absorption coefficient (α), refractive index (n) and band gap values of the copper oxide films.*

Material	λ=600 nm				E_{g1} (eV)	E_{g2} (eV)
	T (%)	R (%)	α $(cm)^{-1}$	n		
BM0	32.53	27.01	5305.38	3.16	1.560	2.040
BM1	22.24	34.77	7211.11	3.87	1.645	2.078
BM3	31.94	27.07	6143.37	3.17	1.641	2.130
BM5	33.47	26.63	5795.12	3.13	1.667	1.952

The optical band gaps of the copper oxide films were determined using the optical method. In this method, the band gap values are obtained by extrapolating the linear portion of the plots of $(\alpha h\nu)^2$ versus $(h\nu)$ to $(\alpha h\nu)^2=0$. The variations are given in Fig 4. As seen from Fig. 4, all films have direct band gaps. Also, it was seen from the plots that all films have two different optical band gaps because there are two linear regions which have different slopes. These energy gaps were calculated as E_{g1} which refers to the band gaps of CuO and E_{g2} which represents those of the Cu_2O. The values are listed in Table 2. As seen from Table 2, E_{g1} values were found to be between 1.560-1.667 eV, and E_{g2} values were found to be between 1.952-2.130 eV.

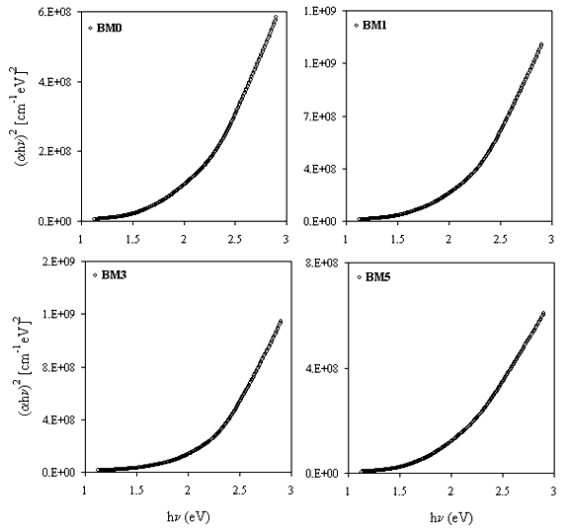

Fig. 4. The plots of $(\alpha h\nu)^2$ versus $(h\nu)$ of the copper oxide films.

3.2. Structural properties

The XRD patterns ($20° \le 2\theta \le 60°$) of the copper oxide films are given in Fig. 5. BM0 films have amorphous structure and high background intensities. But, Mg doped copper oxide films have polycrystalline structures because of the presence of different peaks such as Cu_2O and CuO, and background intensities decreased. Furthormore, the full width half maximums (FWHM, B) decreased by increasing Mg incorporation. So, it was concluded that Mg incorporation improved the crystallinization level of the undoped copper oxide films.

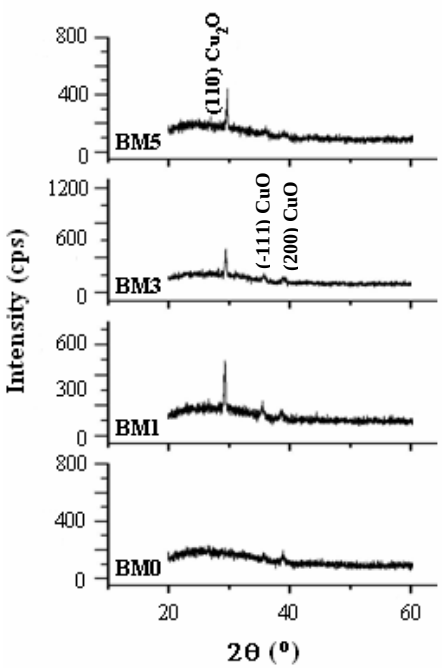

Fig. 5. The XRD patterns of the copper oxide films.

Harris analysis was performed to determine the preferential orientations from XRD data. The texture coefficient was calculated using the equation below [23, 24],

$$P(h_i k_i l_i) = \frac{I(h_i k_i l_i)}{I_0(h_i k_i l_i)} \left[\frac{1}{n} \sum_{i=1}^{n} \frac{I(h_i k_i l_i)}{I_0(h_i k_i l_i)} \right]^{-1} \quad (4)$$

where I_0 represents the standart intensity (ASTM, American Society of Testing Materials), I is the observed intensity of $(h_i k_i l_i)$ plane and n is the reflection number. $P(h_i k_i l_i)$ has to be bigger than one to determine the preferential orientation [25]. To obtain information about the structural properties in detail, the grain size (D) using Schrerrer formula (neglecting peak broadening due to residual stresses in the films) and macrostrain (<e>) for preferential orientations were calculated using the formulas below [26- 28],

$$D = \frac{0.9\lambda}{B\cos\theta} \quad (5)$$

$$< e > = \frac{d - d_0}{d_0} \quad (6)$$

where B is the half peak width of the peak with maximum intensity as radian, D is the grain size, θ is the Bragg angle, λ is the wavelength of light used, d is the interplanar spacing and d_0 is the interplanar spacing without deformation. The diffraction angle (2θ), the interplanar spacing (d), the interplanar spacing without deformation (d_0), miller indices (hkl), crystal systems, texture coefficients (P), grain sizes (D) and macrostrain values (<e>) for Mg incorporated copper oxide films are listed in Table 3. As seen from Table 3, structural parameters changed depending on the Mg incorporation. The texture coefficient values of the peaks at 2θ=29.360°, 29.500° and 29.739° for BM1, BM3 and BM5 films are bigger than one. So, the preferential orientation of Mg doped copper oxide films is through (110) direction, and Cu_2O phase is more dominant than CuO phase. The D values of the films increased and <e> values decreased depending on the increasing Mg incorporation. The increase of the grain size (D) points out the decrease of the grain boundaries and so the amount of defects in the structure. Also, the decrease of the macrostrain (<e>) values indicated that the crystallinization level improved. Besides it was determined from Table 3 that the diffraction angle (2θ) and interplanar spacing (d) of the (110) peak of Mg doped copper oxide films slightly shifted by the Mg incorporation. These variations in positions of the (110) peak imply that all films have strain. From the XRD analyses it was concluded that Mg incorporation plays a significant role in the microstructure and structural properties of the copper oxide films.

Table 3. The diffraction angle (2θ), the interplanar spacing (d), the interplanar spacing without deformation (d_0), miller indices (hkl), crystal system, texture coefficient (P), grain sizes (D) and macrostrain (<e>) values for copper oxide films..

Material	2θ (deg)	d (Å)	d_0 (Å)	(hkl)	Crystal system	P	D (Å)	<e> $\times 10^{-5}$
BM0	Amorphous structure							
BM1	29.360	3.0396	3.02	(110)	Cu_2O	1.932	280	649
BM3	29.500	3.0255	3.02	(110)	Cu_2O	1.809	331	182
BM5	29.739	3.0017	3.02	(110)	Cu_2O	1.751	382	-606

3.3 Electrical properties

To determine the conduction mechanisms depending on the applying voltage and electrical conductivities of the copper oxide films, planar contacts were made by silver paste. For all films, contact length and the distance between two contacts were selected as ~1 mm and ~1.5 mm, respectively. The current values of the copper oxide films were measured at room temperature in the dark by applying voltage values between 10-700 V. The I-V characteristics of the films are shown in Fig. 6. As clearly seen from Fig. 6, the I-V variations of all films are linear, and so the ohmic current mechanism is dominant. In the ohmic region, the number of free carriers is higher than that of the ones injected into the semiconductor. Thus, the free carriers have more effect than the injected ones on the current. The conductivities of the copper oxide films were calculated by two-probe technique and are listed in Table 4. The electrical conductivities of all films are high, and Mg incorporation has not an important effect on electrical properties of the undoped copper oxide films.

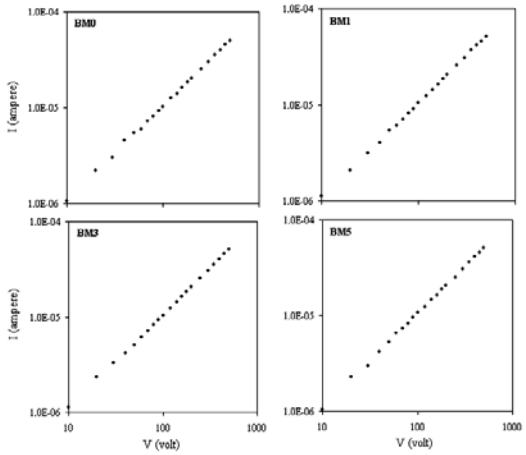

Fig. 6. The I-V characteristics of the copper oxide films.

Table 4. The electrical conductivities of the copper oxide films.

Material	$\sigma \times 10^{-3}$ $(\Omega.cm)^{-1}$
BM0	1.07
BM1	1.13
BM3	1.22
BM5	1.26

4. Conclusions

In this work, the effect of Mg incorporation on the optical, structural, and electrical properties of the ultrasonically sprayed copper oxide films was investigated, and the feasibilities of the films for solar cell devices as absorbing layers were searched. It was clearly seen from optical analyses that Mg incorporation has a strong effect on the optical properties of the copper oxide films. It is well known, copper oxide films are p-type materials; hence their absorption property is a very important optical parameter. In this work, BM1 and BM3 films which have higher absorption coefficients are suitable films for photovoltaic applications as absorbing layer. Also, all films have direct band gaps, and this property is suitable for photovoltaic applications. Besides, the films have two different energy gaps as Eg_1 (the band gaps of CuO) and E_{g2} (the band gaps of Cu_2O). E_{g1} values of the films were found between 1.560-1.667 eV, and E_{g2} values of the films were found between 1.952-2.130 eV. From the structural analyses, it was determined that BM0 films have amorphous structures, while other Mg incorporated copper oxide films have polycrystalline structure. Besides, the crystallinity levels of the copper oxide films improved depending on the Mg incorporation. The electrical investigations showed that for all films, the ohmic current mechanism is dominant in the dark conditions. Besides, the electrical conductivities of all films are high, and Mg incorporation has not a strong effect on electrical properties of the undoped copper oxide films.

Consequently, we can say that Mg incorporation has an affirmative effect on the optical and especially structural properties, and Mg incorporated copper oxide films, especially BM1 and BM3, may be used as absorbing layers for solar cells due to suitable electrical conductivities, high linear absorption coefficient values and good crystalline levels.

Acknowledgements

This work was supported by Osmangazi University Scientific Research Projects Committee under the project number 200419031.

References

[1] E. M. Alkoy, P. J. Kelly, Vacuum **79**, 221 (2005).
[2] K. Tonooka, K. Shimokowa, O. Nishimura, Thin Solid Films **411**, 129 (2002).
[3] A. N. Banerjee, S. Kundoo, K.K. Chattopadhyay, Thin Solid Films **440**, 5 (2003).
[4] S. Ghosh, D. K. Avasthi, P. Shah, V. Ganesan, A. Gupta, D. Sarangi, R. Bhattacharya, W. Assmann, Vacuum **57**, 377 (2000).
[5] S. C. Ray, Sol Energy Mater Sol Cellsi, **68,** 307 (2001).
[6] J. F. Pierson, A. Thobor-Keck, A.Billard, Appl Surf Sci, **210**, 359 (2003).
[7] B. Balamurugan, B.R. Mehta, Thin Solid Films, **396**(1–2)**,** 90 (2001).
[8] J. Morales, L. Sanchez, F. Martin, J. R. Ramos-Barrado, M. Sanchez, Thin Solid Films, **474**, 133 (2005).
[9] J. Morales, L. Sanchez, F. Martin, J. R. Ramos-Barrado, M. Sanchez, Electrochimica Acta, **49**, 4589 (2004).
[10] E. A. Souza, R. Landers, L. P. Cardoso, T. G. S. Cruz, M. H. Tabackniks, A. Gorenstein, Journal of Power Sources, **155**, 358 (2006).
[11] K. H. Yoon, W. J. Choi, D. H. Kang, Thin Solid Films, **372 (1–2)**, 250 (2000).
[12] K. Santra, C. K. Sarker, M. K. Mukherjee, B. Ghosh, Thin Solid Films, **213**, 226 (1992).
[13] M. T. S. Nair, L. Guerrero, O. L. Arenas, P. K. Nair, Appl Surf Sci **150**(1–4), 143 (1999).
[14] A. Y. Oral, E. Mensur, M. H. Aslan, E. Basaran, Mater Chem Phys, **83**(1), 140 (2004).
[15] K. P. Muthe, J. C. Vyas, S. N. Narang, D. K. Aswal, S. K. Gupta, D. Bhattacharya, R. Pinto, G. P. Kothiyal, S.C. Sabharwal, Thin Solid Films **324**, 37 (1998).
[16] M. A. Brookshier, C. C. Chusuei, D.W. Goodman, Langmuir **15**, 2043 (1999).
[17] J. F. Xu, W. Ji, Z. X. Shen, S. H. Tang, X. R. Ye, D. Z. Jia, X.Q. Xin, Solid State Chem **147**, 516 (1999).
[18] F. Atay, V. Bilgin, I. Akyuz, S. Kose, Materials Science in Semiconductor Processing **6**, 197 (2003).
[19] F. Atay, S. Kose, V. Bilgin, I. Akyuz, Materials Letters **57**, 3461 (2003).
[20] J. I. Pankove, Optical Process in Semiconductors, Solid State Physical Electronics Series, Prentice-Hall, N. J., p.422 (1971).
[21] N. Benramdane, W.A. Murad, R.H. Misho, M. Ziane, Z. Kebbab, Mater. Chem. Phys., **48**, 119 (1997).
[22] T. Maruyama, Solar Energy Materials and Solar Cells, **56**, 85 (1998).
[23] C. S. Barrett, T. B. Massalski, Structure of metals, Oxford: Pergamon, p. 204 (1980).
[24] V. Bilgin, S. Kose, F. Atay, I. Akyuz, Journal of Materials Science, **40**, 1909 (2005).
[25] J. P. Nair, R. Jayakrishnan, N. B. Chaure, R. K. Pandey, Semiconductor Science and Technology, **13**, 340 (1998).
[26] Jr. R. Mamazza, D. L. Morel, C.S. Ferekides, Thin Solid Films **484**, 26 (2005).
[27] R. Ferro, J. A. Rodriguez, O. Vigil, A. Morales-Acevedo, Materials Science and Engineering B, **87**, 83 (2001).
[28] W. D. Callister, Materials Science and Engineering – An Introduction, John Wiley and Sons, New York, (1997).

*Corresponding author: fatay@ogu.edu.tr